

# Superplastic deformation and microstructure evolution in PM IN-100 superalloy

SHIOMI KIKUCHI, SHOUSAKU ANDO, SHU FUTAMI, TATSUO KITAMURA, MASAHIRO KOIWA

*Department of Metal Science and Technology, Kyoto University, Sakyo-ku, Kyoto 606, Japan*

The superplastic deformation behaviour of PM IN-100 alloys consolidated by hot isostatic pressing (HIP) was investigated in compression tests at temperatures between 1323 and 1373 K. The microstructural changes were observed using scanning electron microscopy. In the high strain rate region, grain refinement occurs due to dynamic recrystallization, resulting in the work softening type stress-strain curves. At low strain rates, grain growth occurs during deformation corresponding to work hardening. The strain rate sensitivity index,  $m$ , reaches a maximum value ( $m = 0.6$ ) at the optimum strain rate which depends on the test temperature. The grain size dependence coefficient,  $p$ , was determined to be 2.0. The activation energy for deformation was  $348 \text{ kJ mol}^{-1}$ . The rate-controlling mechanism of superplasticity in as HIPed IN-100 seems to be the grain-boundary sliding controlled by volume diffusion rather than grain-boundary diffusion.

## 1. Introduction

Powder-consolidated materials are receiving much attention for structural applications at elevated temperatures. Jet engine parts such as turbine discs can be manufactured from nickel-base superalloys by the combination of powder metallurgy (PM) and superplastic forming techniques. The most famous superplastic forming process is known as "Gatorizing" in which PM consolidates are heavily worked by extruding at elevated temperatures and then heated at a temperature just above the recrystallization temperature to obtain fine-grained structure. The materials made in this process can be deformed superplastically by lower strain rate forging.

A number of investigations [1-5] on the superplastic behaviour of nickel-base superalloys have been reported in the literature. Menzies *et al.* [1, 2] studied the superplastic deformation behaviour and microstructural changes in powder-consolidated IN-100. Their results showed that the deformation behaviour can be divided into three characteristic regions depending on strain rates. At low strain rates (Region I) the strain rate sensitivity is low and work hardening occurs. At intermediate strain rates (Region II) the strain rate sensitivity index  $m$  is larger than 0.6 and work softening is observed. The optimum superplasticity can be attained in this region. At high strain rates (Region III) the value of  $m$  becomes smaller again. They have concluded that in Regions I and II the deformation takes place by grain-boundary sliding with accommodation by both slip and diffusion. Deformation in Region III produces grain refinement accompanied by a marked increase in dislocation density and some cavitation.

The above observations are very significant from a technological point of view. Firstly, the larger strain

rate sensitivity at high strain rates implies a possibility of superplastic forming at a high strain rate, which is favoured in production. Secondly, the grain refinement which is usually achieved by pretreatments, may be accomplished during the deformation process, which is also expected to reduce the production cost.

Most of the investigations reported on the superplastic deformation in PM IN-100 alloys have been done for the as-extruded materials. In this investigation, we examine the superplastic behaviour of PM IN-100 alloys consolidated by hot isostatic pressing (HIP). The optimum conditions of temperature and strain rate for superplastic deformation are determined and the effect of the structural changes during deformation on the superplastic behaviour is described.

## 2. Experimental procedure

The alloy used in this study was a powder metallurgy nickel-based superalloy IN-100 with composition as given in Table I. The powder, under 350 mesh, which had been argon atomized, was loaded into stainless steel cans, and sealed in a vacuum by electron-beam welding. The canned powder was consolidated by hot isostatic pressing (HIP) under an argon atmosphere of 150 MPa for 2 h at 1373 K.

Specimens for compression tests were machined from the compacted rods to 4 mm diameter and 10 mm long. All specimens for the mechanical test were as hot-pressed materials (as HIPed). Compression testing was carried out in vacuum at 1323, 1348

TABLE I Chemical composition of IN-100 (wt %)

Ni	Cr	Mo	Co	Ti	Al
bal.	12.38	3.53	18.52	4.26	4.90

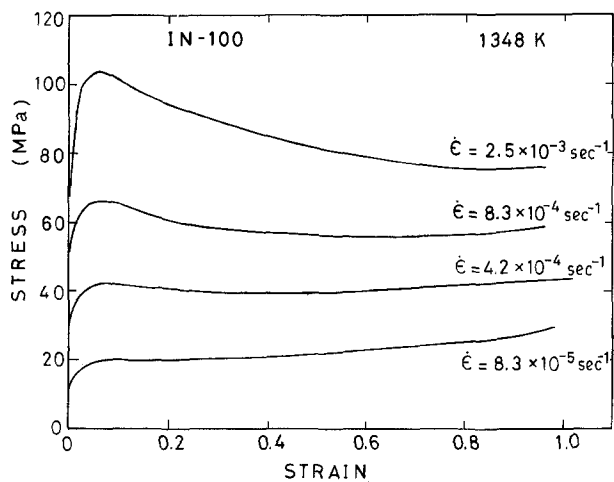


Figure 1 True stress — true strain curves at 1348 K.

and 1373 K with the initial strain rate ranging from  $8.3 \times 10^{-5}$  to  $4.2 \times 10^{-3} \text{sec}^{-1}$  using an Instron-type machine with constant cross-head speed. The specimens were compressed between TZM (Mo alloy) plates. The glass lubricant was used in order to decrease the friction of the contact surface. The deformed specimens were rapidly cooled to room temperature to freeze-in the microstructure.

Microstructure was observed using a scanning electron microscope (SEM, Hitachi S450) at 20 kV. Specimens were polished and etched with a mixture of 80 ml HCl, 2 ml HNO<sub>3</sub>, 11 ml water and 16 g FeCl<sub>3</sub> at 353 K.

### 3. Results and discussion

#### 3.1. Flow behaviour in compression

Fig. 1 shows the true stress — true strain curves for as-HIPed specimens of IN-100 obtained at various initial strain rates at 1343 K. Two types of flow behaviour, work hardening and work softening, were observed. At high strain rates, the flow stress rapidly increases to a maximum at a strain of several per cent and then gradually decreases with strain, i.e. work softening behaviour. In the low strain rate region, the flow stress shows a steady state deformation stage where flow stress maintains a constant level, and is followed by the work hardening stage.

The strain rate of the transition from work hardening to work softening depends on test temperature; it increases with the increase in temperature.

#### 3.2. Microstructures after deformation

Fig. 2 is a scanning electron micrograph of as-HIPed material (starting material), which essentially consists of  $\gamma$  and  $\gamma'$  phases. The volume fraction of  $\gamma'$  phase is about 60%. The dark regions in the micrograph are  $\gamma'$  phase. The oxide layers are observed along the boundaries between consolidated powder particles. The grain size is not uniform but ranges from 1 to 7  $\mu\text{m}$ ; the average grain size of the starting material is 3  $\mu\text{m}$ .

Figs 3a and b show the microstructure after deformation to a strain of 1.2 at a strain rate of  $2.5 \times 10^{-3}$  and  $8.3 \times 10^{-5} \text{sec}^{-1}$ , respectively. At high strain rate (Fig. 3a), the grains become finer during deformation. The grain size in the initial state has a wide distribution, but after large amounts of strain it

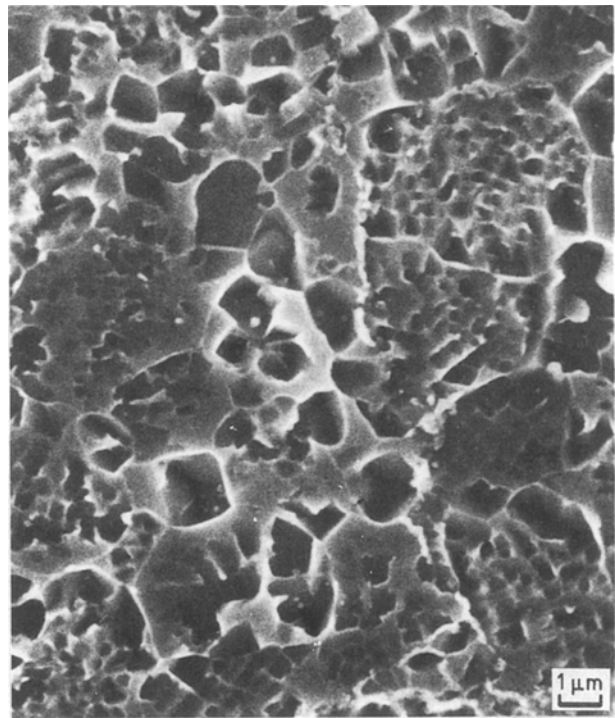


Figure 2 A scanning electron micrograph of the as-HIPed material.

becomes uniform. This result indicates that dynamic recrystallization occurs during superplastic deformation. The  $\gamma'$  phases within the  $\gamma$  grains remain fine after deformation. The proportion of  $\gamma'$  phases existing on the grain boundaries between  $\gamma$  grains is very low, and most of them are inside the  $\gamma$  grains. At the low strain rate (Fig. 3b), the grains are coarsened by grain growth during deformation, and especially an agglomeration of  $\gamma'$  phases within the  $\gamma$  grain was noted. The amount of  $\gamma'$  phases at grain boundaries consequently increases. From Figs 3a and b it can be seen that the  $\gamma$  grain remains equiaxed after deformation although the grain growth or refinement takes place. This means that the deformation mainly occurs by grain-boundary sliding.

In order to visualize clearly the trend of grain-size variation after deformation under varying conditions, the average grain sizes after 1.2 strain are indicated in Fig. 4, as functions of temperatures and strain rates. The region of about 3  $\mu\text{m}$ , which is the same as that for the starting material forms a narrow band; with the increase in temperature, the range shifts towards higher strain rates. Note that in this region, the microstructure does change during deformation, keeping the same average grain size but resulting in a more uniform grain size distribution, which is attained at a relatively small strain of 0.1. In the upper region, the grain refinement occurs due to dynamic recrystallization, while in the lower region, the grain coarsening occurs.

The microstructural changes observed in the present experiment on as-HIPed IN-100 are essentially similar to those observed by Menzies *et al.* [2] for as-extruded IN-100.

#### 3.3 Stress-strain rate relations

In superplastic metals, the flow stress dependence on strain rate is usually described by the following

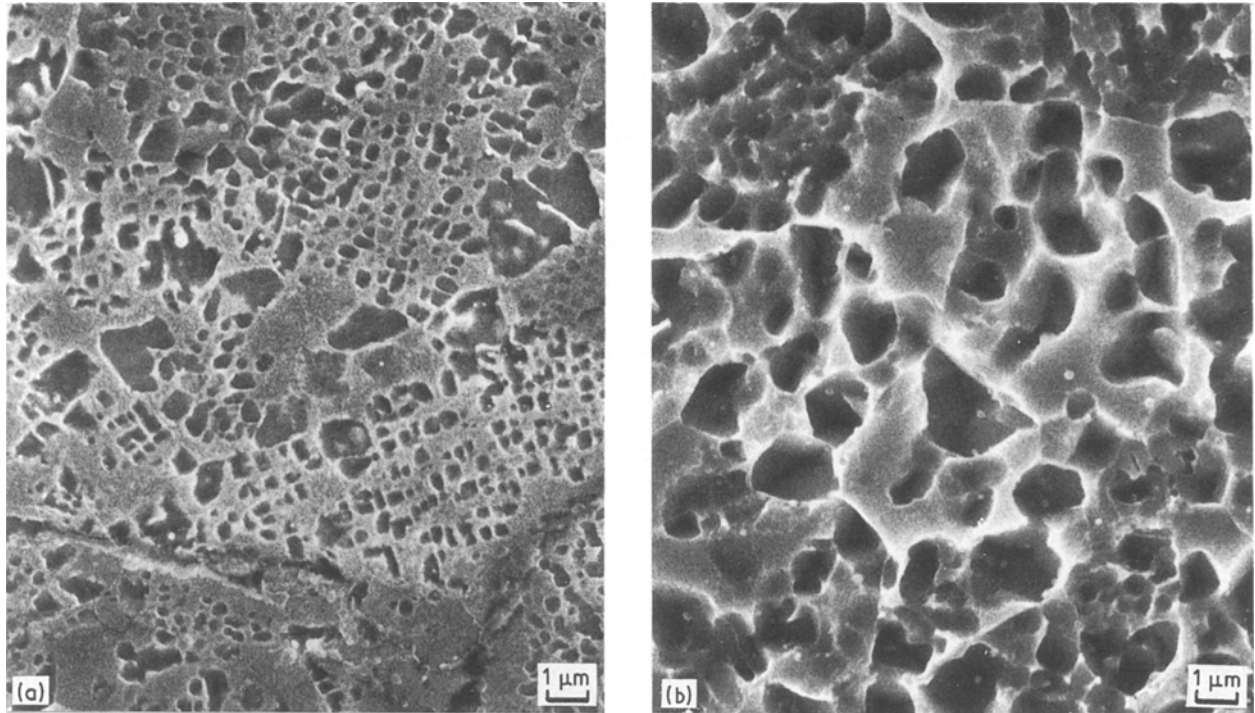


Figure 3 Microstructures after a strain of 1.2 deformed at 1348 K: (a)  $\dot{\epsilon} = 2.5 \times 10^{-3} \text{ sec}^{-1}$ ; (b)  $\dot{\epsilon} = 8.3 \times 10^{-3} \text{ sec}^{-1}$ .

empirical expression [6]

$$\sigma = B\dot{\epsilon}^m \quad (1)$$

where  $\sigma$  is the flow stress,  $\dot{\epsilon}$  is the strain rate,  $B$  is a constant which incorporates the dependence on temperature and  $m$  is the strain rate sensitivity index.

In order to estimate the magnitude of  $m$  for varying conditions,  $\log \sigma$  is plotted as a function of  $\log \dot{\epsilon}$  in Fig. 5. The values of  $\sigma$  are taken from the stress-strain shown in Fig. 1;  $\sigma$  is taken to be the maximum stress for work softening-type curves, and the steady state stress for work hardening-type. The resulting relations are characterized by the sigmoidal curves and divided into three regions of flow which are termed Region I at low strain rates, Region II at intermediate strain rates where the flow behaviour is superplastic, and Region III at high strain rates.

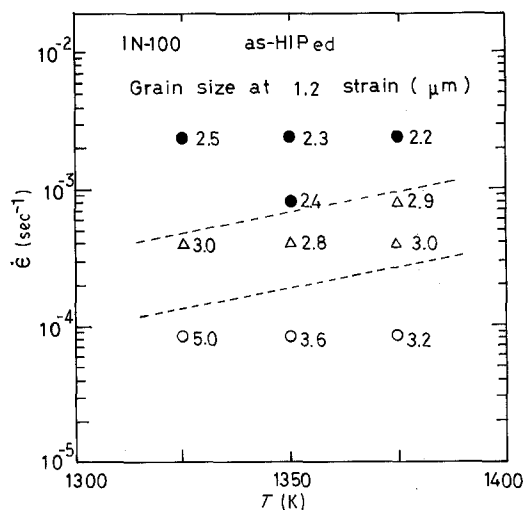


Figure 4 Grain sizes of specimens deformed to a strain of 1.2 at various strain rates and temperatures. (●) Refined, (Δ) unchanged, (○) coarsened.

The relationship between the strain rate sensitivity index,  $m$ , and strain rate,  $\dot{\epsilon}$ , was derived from the  $\log \sigma - \log \dot{\epsilon}$  plot in Fig. 5 and the results are shown in Fig. 6. The values of  $m$  obtained invariably show a maximum at some optimum strain rate, decreasing at both higher or lower strain rates than the optimum one. The values of  $m$  vary within 0.3 to 0.6. The optimum strain rate in Region II depends on the test temperature and shifts towards the higher strain rate with increasing temperature. At 1373 K,  $m$  is about 0.5 even in the strain-rate range of  $10^{-2} \text{ sec}^{-1}$ . These results indicate that from the technical point of view, the as-HIPed materials of IN-100 should be deformed at higher temperatures but below the  $\gamma'$  solvus. If  $\gamma'$  phase is dissolved, the superplasticity cannot be expected, because grain growth occurs and the microstructures with fine grains are not maintained.

### 3.4. Grain-size dependence on strain rate

Most of investigations [7-11] on the superplastic deformation of materials with micrograins suggest

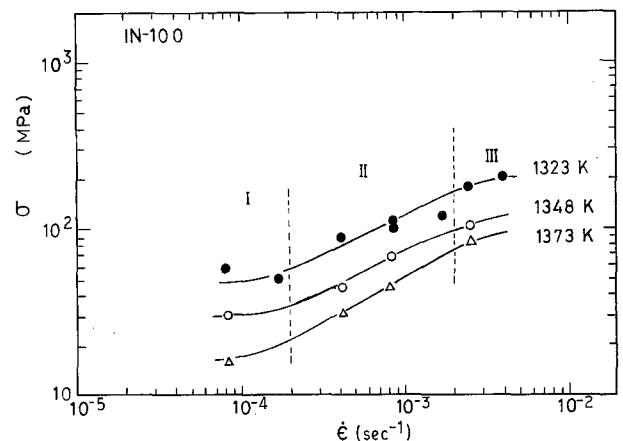


Figure 5 Strain-rate dependence of flow stress in as-HIPed IN-100.

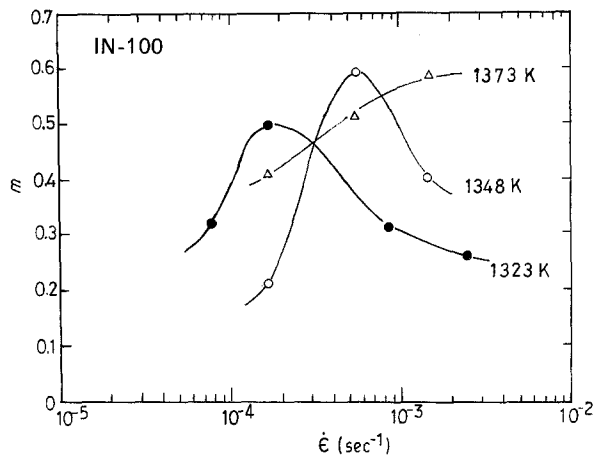


Figure 6 Variation of  $m$  with strain rate.

that grain-boundary sliding is the dominant mechanism in the deformation process. In this case the grain size remarkably affects the strain rate or the flow stress. The empirical rate equation including the grain-size dependence of superplasticity can be given by [12]

$$\left(\frac{\dot{\epsilon}kT}{DGb}\right) = A\left(\frac{b}{d}\right)^p\left(\frac{\sigma}{G}\right)^{1/m} \quad (2)$$

where  $k$  is the Boltzmann constant,  $T$  the absolute temperature,  $D$  the diffusion coefficient,  $G$  the shear modulus,  $b$  the length of the Burgers vector,  $A$  a structural constant,  $d$  the grain size, and  $p$  and  $m$  are constants. The grain-size dependence coefficient  $p$  will vary between 0 and 3 depending on the deformation mechanism; the value of  $p$  for the most typical superplasticity is 2.

In order to determine the value of  $p$ , one naturally requires specimens of different grain sizes. As shown in Fig. 4, specimens of different grain sizes can be prepared by deforming under various temperatures and strain rates. Such specimens were further subjected to deformation at 1232 K at a constant initial strain rate of  $4.1 \times 10^{-4} \text{ sec}^{-1}$ . A schematic illustration of this test is given in Fig. 7. The flow stress at 0.2% strain,  $\sigma_{0.2}$ , was conveniently taken, and plotted as a function of the grain size,  $d$ , in Fig. 8. The linear relation on log-log plot of flow stress against grain size indicates that the product of  $m$  and  $p$  is a constant

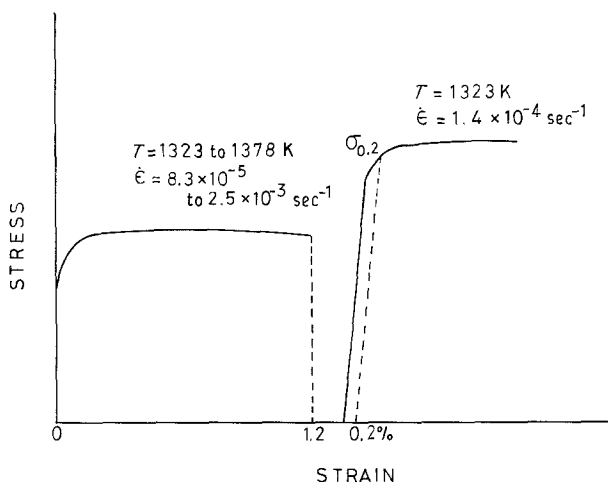


Figure 7 A schematic illustration to obtain the grain-size dependence of flow stress.

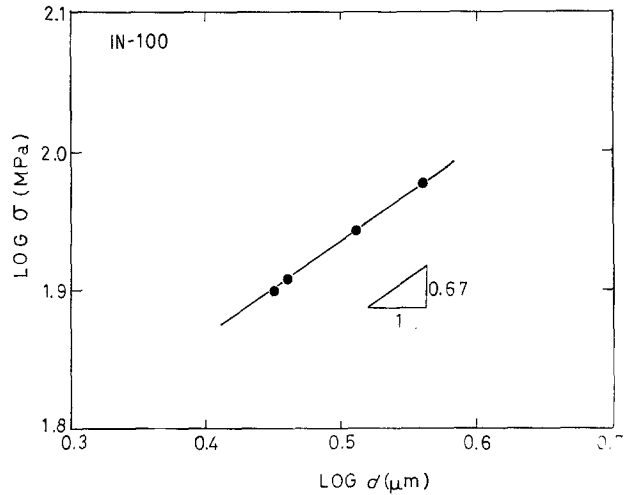


Figure 8 Effect of average grain size on the flow stress at a strain rate of  $4.1 \times 10^{-4} \text{ sec}^{-1}$ .

as predicted from Equation 2. From Fig. 8,  $mp = 0.67$  was obtained.

It is evident from the above results that the value of  $m$  varies with strain rate, temperature and also microstructure. For the determination of  $p$ , it is necessary to specify the value of  $m$ . Although  $m$  may be estimated from Fig. 5, it is not suitable, because those data are obtained from the starting materials. Therefore in order to determine  $m$  for the same deformation conditions at which the grain-size dependence of flow stress was obtained, strain rate change tests were carried out for the deformed specimens. The average value of  $m$  determined from the strain rate change test method is 0.34, and consequently the grain-size dependence coefficient  $p$  has a value of 2.0. This is in good agreement with the values reported in the literature [12] and is as expected from the existing theoretical models [12] for superplasticity.

### 3.5. Activation energies for deformation

The activation energy,  $Q$ , for deformation can be determined from relative displacement of log strain rate-log flow stress curves in Fig. 5. The value of  $Q$  for Region II is  $348 \text{ kJ mol}^{-1}$ .

The activation energies for superplastic deformation of IN-100 reported by other investigators and the results of the present investigation are given in Table II. It should be noted that most of the activation energies reported for superplasticity of IN-100 are much larger than the present value except the result of Torisaka *et al.* [15]. In general, for micrograin superplastic materials, the activation energy for deformation is the same as that for grain-boundary diffusion, and the rate-controlling process is considered

TABLE II Activation energies for superplastic deformation of IN-100

$Q$ (kJ mol <sup>-1</sup> )	Grain size (μm)	Reference
399	1.3	[5]
412	13	[13]
350	25	[14]
483	2.7	[1]
344	3.9	[15]
348	3	Present investigation

to be grain-boundary sliding controlled by grain-boundary diffusivity. However, the activation energy obtained in this experiment is much higher than that of the grain-boundary diffusion, which is usually about half the activation energy for lattice diffusion. Therefore, the superplastic deformation of the as-HIPed materials of IN-100 seems to be controlled by the lattice diffusion.

In complex alloys such as used in the present experiment, it is not clear the diffusion of which element is controlling the flow behaviour. Several activation energies for volume diffusion are given in the literature: nickel in nickel 285 kJ mol<sup>-1</sup> [16]; cobalt in nickel 269 kJ mol<sup>-1</sup> [17]; chromium in nickel 285 kJ mol<sup>-1</sup> [18]; nickel in Ni-Cr 280 to 294 kJ mol<sup>-1</sup> [19]; chromium in Ni-Cr 284 to 295 kJ mol<sup>-1</sup> [19]. The value of 348 kJ mol<sup>-1</sup> obtained in the experiment is higher than the above activation energies, but may be regarded as that for volume diffusion.

From the present results, it can be considered that the superplastic deformation of IN-100 is attributed to the combined action of grain-boundary sliding and deformation of the  $\gamma$  phase which is softer than the  $\gamma'$  phase. The grain-boundary sliding is accommodated by dislocation motion in which the rate-controlling step is the climb of dislocations in the  $\gamma$  phase.

#### 4. Conclusions

For the as-HIPed materials of IN-100, the superplastic behaviour has been investigated in compression tests. The following results were obtained.

1. The stress-strain behaviour can be classified into two types, work softening at high strain rates and work hardening at low strain rates.

2. In the high strain rate region, the grain refinement occurs during deformation due to dynamic recrystallization, resulting in the work softening type stress-strain curves. At low strain rates, the grain growth occurs during deformation corresponding to work hardening.

3. The strain rate sensitivity index,  $m$ , becomes a maximum value at the optimum strain rate which depends on the test temperature. The maximum value of  $m$  obtained is 0.6.

4. The grain-size dependence coefficient,  $p$ , is determined to be 2.0, which is in good agreement with the value expected in superplastic deformation.

5. The activation energy for deformation is 348 kJ mol<sup>-1</sup>. The rate-controlling mechanism of superplasticity in as-HIPed IN-100 seems to be grain-boundary sliding controlled by volume diffusion rather than grain-boundary diffusion.

#### Acknowledgements

The authors thank Mr Y. Takeda and Mr N. Uenishi, Sumitomo Electric Industries Ltd, for supplying the alloy, and Mr I. Nakagawa for the SEM work. This research was supported in part by the Grant-in-Aid of the Ministry of Education, Science and Culture of Japan (no. 63 550 535).

#### References

1. R. G. MENZIES, J. W. EDINGTON and G. J. DAVIES, *Metal Sci.* **15** (1981) 210.
2. R. G. MENZIES, G. J. DAVIES and J. W. EDINGTON, *ibid.* **16** (1982) 483.
3. *Idem*, *ibid.* **16** (1982) 356.
4. J.-P. A. IMMARIGEON and P. H. FLOYD, *Met. Trans.* **12A** (1981) 1177.
5. S. H. REICHMAN and J. W. SMYTHE, *Int. J. Powder Met.* **6** (1970) 65.
6. P. K. PADMANABHAN and G. J. DAVIES, in "Superplasticity" (Springer Verlag, Berlin 1980).
7. T. G. LANGDON, *Metals Forum* **4** (1981) 14.
8. J. W. EDINGTON, *ibid.* **4** (1981) 63.
9. M. F. ASHBY and R. A. VERRALL, *Acta Metall.* **21** (1973) 149.
10. A. BALL and M. M. HUTCHISON, *Met. Sci. J.* **3** (1969) 1.
11. R. C. GIFKINS, *Met. Trans.* **7A** (1976) 1225.
12. A. ARIELI and A. K. MUKHERJEE, *ibid.* **13A** (1982) 717.
13. L. M. MOSKOWITZ, R. M. PELLOUX and N. J. GRANT, in "Proceedings of the Second International Conference on Superalloy Processing" (Metals and Ceramics Information Centre, Columbus, Ohio 1972).
14. Y. KOBAYASHI, MS thesis, Massachusetts Institute of Technology (1974).
15. Y. TORISAKA, Y. NAKAZAWA and M. MIYAGAWA, *Tetsu to Hagane* **72** (1986) 1567 (in Japanese).
16. H. BAKKER, *Phys. Status Solidi* **28** (1968) 569.
17. M. BADIA and A. VIGNES, *Acta Metall.* **17** (1969) 177.
18. A. R. PAUL, M. C. MURTY and S. W. ZEHR, *J. Nucl. Mater.* **58** (1975) 205.
19. J. RUZICKOVA and B. MILLION, *Mater. Sci. Engng* **50** (1981) 59.

Received 6 June

and accepted 23 October 1989